EUROPEAN ORGANIZATION FOR NUCLEAR RESEARCH

CERN-EP/90-11
January 23rd, 1990

A NEW MICROSTRIP DETECTOR WITH DOUBLE-SIDED READOUT

B.S. Avset, L. Evensen
SI, Oslo, Norway

V. Chabaud, H. Dijkstra, R. Horisberger, L. Hubbeling, G. Maehlum,
A. Peisert, I. Roditi and P. Weilhammer
CERN, Geneva, Switzerland

A. Czermak, P. Jalocha and M. Turala
Institute of Nuclear Physics, Cracow, Poland

Ph. Bambade
LAL, Orsay, France

W. Dulinski, R. Turchetta and M. Schaeffer
CRN, Strasbourg, France

M. Battaglia
INFN, Milan, Italy

Iiro Hietanen and T. Tuuva
University of Helsinki, Helsinki, Finland

Presented by P. Weilhammer at the 1989 IEEE Nuclear Science Symposium

Abstract

A Si μ-strip detector has been developed with 50 μm pitch strips on both p- and n-side, using the principle of capacitive coupling between p^+ diode strips - respectively n^+ strips and the metallization strips which connect to the front-end preamplifiers. The detector is biased on both sides via polysilicon resistors connecting each p^+ or n^+ line to a common bias bus. To allow ohmic separation at the n-side, the accumulation layer of electrons has to be disrupted between the n^+ strips. This has been achieved in three different ways : i) separate polysilicon lines on thick oxide between two adjacent n^+ lines to break the conducting accumulation layer by externally induced field depletion or using the metal lines of the n^+ strips ii) on thick oxide and iii) on thin oxide. Results on 20×20 mm^2 test devices will be presented.

1. INTRODUCTION

Considerable expertise in the use of high spatial resolution μ-strip detectors with readout on the p-side in high energy physics experiments has been obtained [1]. Projects to build μ-vertex detectors for collider experiments using p-side readout Si strip detectors are well advanced [2]. The DELPHI μ-vertex detector with 2 concentric shells of strip detectors with rφ readout (with 5120 channels out of 30,720 channels total on outer layer, with all 24,576 channels on inner layer) and a detector spatial resolution of $\sigma_{r\phi}$ = 5 μm [3] has been inserted into the DELPHI experiment.

A natural extension of the single sided strip detector is to pattern the back side of the detector to get space point information. Although this may seem simple, one will soon face the problems encountered with strip detectors made on p-type material. Fixed positive charges which are always present in SiO_2 at the oxide-Si interface create an accumulation layer of negative charges in the n-type silicon which leads to an ohmic connection of the n-strips, destroying position information. By surrounding the n^+-strips with a p^+-type implantation, isolation can be achieved.

Detectors with readout on p- and n-side at the same time based on this idea have recently been built and tested [4]. They will be used in the Minivertex Detector for the ALEPH experiment at LEP [5], the most ambitious collider vertex detector project so far undertaken with 2 layers of detectors around the beam pipe, each with rφ and z readout.

Our approach is based on a MOS structure which is naturally available in capacitively-coupled Si μ-strip detectors. If two phosphorus-doped areas in an n-type substrate are separated by an oxide with metal gate, one can control the current flowing between the two contacts with the gate voltage. By choosing the correct polarity and voltage between gate and substrate, a field-induced junction can be made which

will isolate the two regions. This is the basis for one of the designs, in which we use polysilicon field-plates in between n^+-strips.

Another and simpler design exploits the dielectric isolation of the aluminium readout line which can be biased independently of the rest of the device. By extending the readout line sideways beyond the n-strip, the same MOS gate structure has been created. Under proper operating conditions, two field-induced junctions are created which isolate neighbouring n-strips. To investigate this scheme two different designs were made. In the next section we describe the lay-outs of the three types of detectors. In section 3 processing is described and sections 4 and 5 give results of electrical measurements and tests with the VLSI electronics.

2. DESIGN

Based on a capacitively coupled silicon microstrip detector [6], a single layout was designed for the front side with a 10 μm wide p-type line and 50 μm pitch. The active area of the detector is surrounded by a 300 μm wide guard ring. The chip size is 22.5 mm by 22.5 mm and has a 2 mm wide boundary for mounting. Bias is provided through individual polysilicon resistors between the strip and the bias bus line. All strips are biased in parallel with a single connection to the bias bus line. Leakage current from the whole active area of the detector can be measured on the bias line. Aluminium readout lines are capacitively coupled with SiO_2 as dielectric to the p-side of the pn-junction. The strip pitch of 50 μm on the p-side for this prototype device was chosen for convenience. For experimental applications where very high spatial resolution is required, the p-side strips can be laid out with a 25 μm pitch, as has been done for the DELPHI μ-vertex detector [7]. Spatial resolution with such detectors of σ = 3.2 μm to 3.5 μm has been achieved in a test beam [6].

The front side design was the starting point for the back side. The n-strips are 10 μm wide with a pitch of 50 μm and oriented orthogonal to the front side strips. Again considerations to achieve the best possible spatial resolution were left aside in the design and will be implemented once the feasibility of the method has been demonstrated. Bias and readout is done in the same way as on the front side. All n-strips are connected to a common bias bus line with individual polysilicon resistors and coupled capacitively to the the readout line. Three designs were made for the field-induced junction (Figure 1). Design A (Fig. 1a) has a separate polysilicon gate on top of the oxide in between the n-strips. Since the gate width is a free parameter, we have divided the detector into 3 regions with 128 strips each with 10 μm, 20 μm and 30 μm polysilicon line widths. The gate line can be biased independently of all other functions of the detector and allows the exploitation of the full range of field-induced isolation.

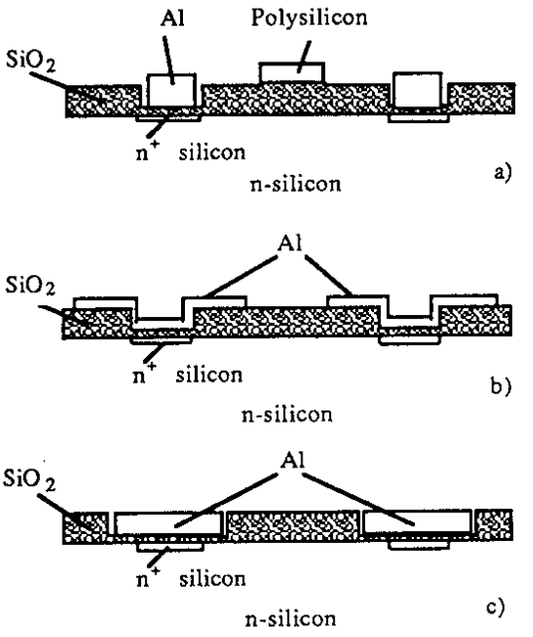

Fig. 1

The two other designs exploit directly the MOS features of the readout lines. Both these designs have a metal line extending sideways outside the n-strip. The design B (Fig. 1b) has no extra masks or processing steps with comparison to the p-side. This would be the simplest approach to put into production and should offer the highest yield.

Again as for design A, we implemented three different widths of metal lines, 20 μm, 30 μm, 40 μm.

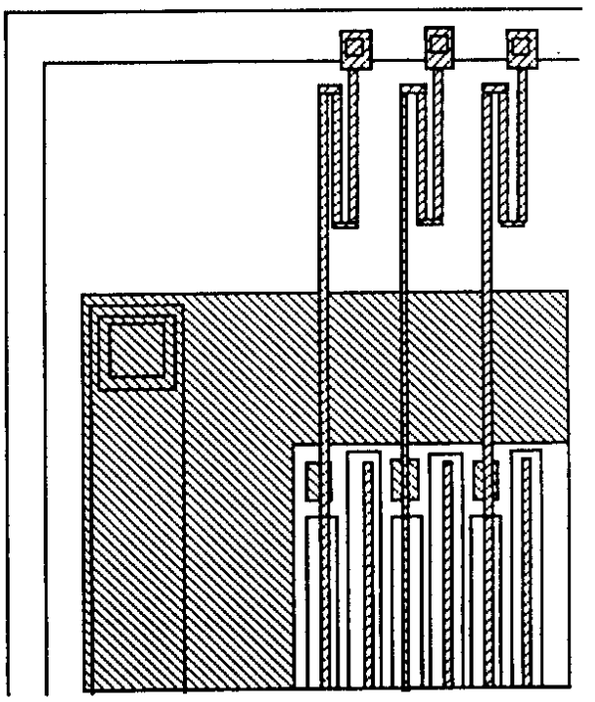

Fig. 2

Another variation, design C, (Fig. 1c), has a thin oxide extending sideways beyond the n-strip with the metal readout line covering the whole width of the thin oxide. The reason for this approach is to be able to study the effect of stronger depletion fields for the case of narrow metal lines. The thin oxide region requires an extra etching mask and processing step. The line widths are 15 μm, 25 μm and 35 μm in the 3 regions. Figure 2 shows the layout of one corner of the design shown in Fig. 1b.

Special test structures together with process monitors were included on the final mask layout. One test structure was designed to test the front surface design and has a large n-contact on the back side. Another test design has a large pn-junction on the front side, together with the most promising back side design. The mask set consists of 11 masks, all made with optical pattern generation.

3. PROCESSING

n-type, phosphorus-doped wafers with both sides polished were chosen as substrate material. The resistivity was approximately 5000 Ωcm, thickness 280 μm with <100> orientation and 3 inch diameter. Prior to the first oxidation process, all wafers were RCA cleaned [6]. A combination of HC_2 and wet oxidation was used to grow a 1 μm thick field oxide. Standard photolithography defined the oxide openings for the n-strips on the back side, where phosphorus was deposited by gas phase deposition using PH_3 at 1100°C. The phosphorus layer was diffused in combination with an oxidation step.

Front to back side alignment was done using an IR alignment system at the same time defining the oxide openings for the p-strips on the front side. Gas phase deposition of boron from diborane was used to obtain pn-junctions. After etching of the boron glass, boron was diffused and the first part of the coupling oxide was grown. Contact holes were opened on both sides of the wafer prior to LPCVD polysilicon deposition. The polysilicon was ion implanted with boron to give a sheet resistivity of 15 kΩ/square. The polysilicon pattern was defined by photolithography and etched in a barrel reactor using CF_4. An oxide passivation layer was grown on the polysilicon, at the same time defining the final thickness of the coupling oxide.

Two photolithography steps opened contact holes on both sides prior to E-gun evaporation of aluminium. Aluminium lines were patterned with standard lithography and wet etching. As a final step the wafers were annealed in forming gas (N_2 + H_2) at 450°C to reduce the oxide charge and alloy the aluminium in the contact holes.

4. ELECTRICAL MEASUREMENTS

A batch of 20 wafers with 4 useful 22×22 mm^2 detectors on each wafer (2 detectors of design 1 and 1 detector of design 2 and 3 each) has been processed. For reasons which are fully understood now, the polysilicon resistors had lower resistance than initially specified in the design. First results on electrical measurements from some of the detectors are presented in the following.

A. Leakage Current

Reverse bias currents are measured with the n-side bias pad and guard ring connected together and put on positive voltage. The p-side bias and guard ring current are monitored separately. Most detectors tested have reverse currents of several tens of μA for the whole detector. Separate contact pads allow to measure the current from single strips. We find that the current is distributed rather uniformly over all strips. A few detectors have low leakage currents. Figure 3 shows the leakage current on the bias line and the guard ring of a detector of design 2. Though average leakage currents per strip allow to use these detectors for particle detection, the processing has to be improved to limit reverse bias currents to less than 2 μA for the whole detector.

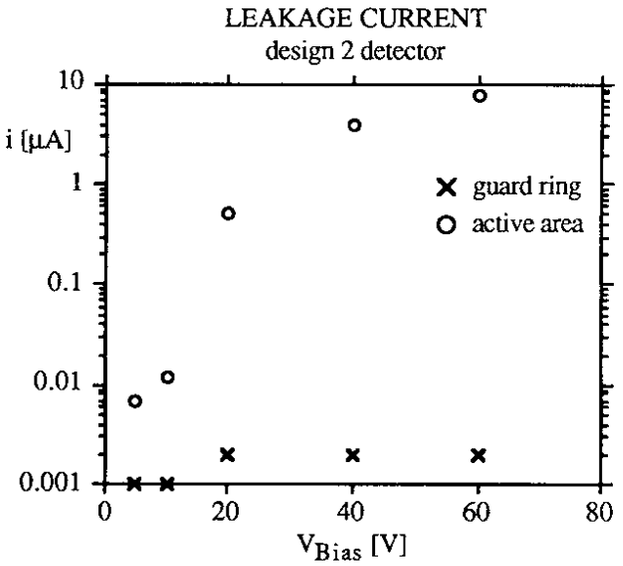

Fig. 3

B. Ohmic Separation of Strips on n-Side

We expect to achieve high ohmic resistance between two n^+ strips, once the detector is fully depleted through to the n-side (about 60 V between p-n junction and the n^+ strips), by creating a field-induced junction through a negative voltage at the readout metal strips or the polysilicon field plates. Increasing this negative potential on the gates will create a fully depleted zone in between the n^+ strips.

Measurement of the interstrip resistance R_i is not straightforward, because all strips are connected to the common bias line through polysilicon resistors, R_p. We adopted an indirect method of measuring the resistance between the bias line and a contact hole on one strip, by applying a voltage and measuring the induced current. The measured resistance, Rm, is a convolution of 384 parallel resistors, each being a combination of Rp and Ri. Knowing the value of Rp, we can deduce

Ri. We have performed this measurement on the three regions with different line widths on the three types of detectors as a function of the gate voltage. In the case of design 1 detector, we applied the polarizing voltage to the polysilicon field plates and on design 2 and 3 detectors to the aluminium readout lines. Figure 4 shows the deduced interstrips resistance for the three designs and for 20, 20 and 35 μm lines for design 1, 2 and 3 respectively. For the other regions we obtained a similar dependence. We can see that at a polarizing voltage of a few volts, the interstrip resistance reaches more than 100 MΩ.

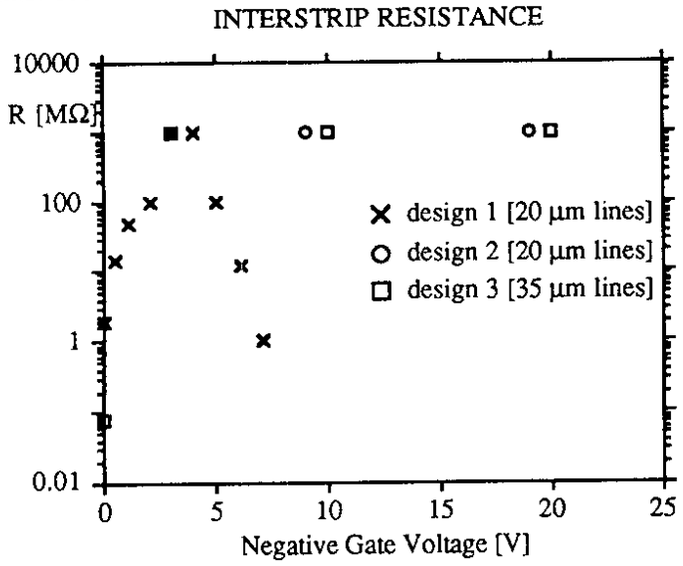

Fig. 4

C. Capacitances

For a good performance of the detectors, the coupling capacitance between p^+ resp. n^+ strips and the metallization strips should be large w.r.t. the capacitance to side strips, in order to collect as much as possible of the signal on the readout strips. For present designs the capacitance between p^+ and n^+ side can be neglected. The capacitance to the neighbouring strips represents the capacitance to the effective ground and represents therefore essentially an important contribution to the noise of the preamplifier. It therefore should be as small as possible.

For these prototype detectors, optimization was tried in view of good signal collection properties on the n^+ side more than for optimal layout to achieve low interstrip capacitances. Quantitative results for these detectors are not yet available. For the final design one should aim for as narrow as possible field plates.

5. TEST OF DETECTORS WITH VLSI READOUT

The design of these detectors aims for readout of the induced charge with VLSI chips. The MX3 CMOS chip [9] with a charge-sensitive preamplifier for each channel, two storage capacitors for double-correlated sampling and a shift register for multiplexed readout was used. Making full use of the capacitive coupling we put the readout electronics on both sides of the detector on ground potential, having +4.2 V on the input of the preamplifiers [8]. For the final design it is foreseen to bias the p-side with a voltage of a few hundred millivolt above the input of the preamplifier and the n-side at the full positive bias voltage. Such polarization reduces the sensitivity to radiation [9] and gives the correct field-plate voltage for n^+ ohmic separation. For the present design we have encountered some difficulties to put full positive bias voltage (~ 60 V) on the n-side strips because of too small distances between the aluminium readout strips and bond wires to the contact holes of polysilicon resistors which caused occasional shorts. In the next design the distance of the contact windows and the first bond row will be increased.

Two different detectors were used in this test, one of design C and one of design B. Both detectors were connected on both sides to 3 readout chips using a ceramic frame mounting. The chips were glued onto a ceramic hybrid [11], which is part of the ceramic frame. Via this hybrid the clock signals could be brought to the chips and the signals were sent by a wideband video amplifier via a twisted pair to a flash ADC [11]. Whereas the detector of design B could be mounted without creating a single short between an n^+ strip and its metal readout-line, the detector of design C had a few shorts after mounting on both the n- and the p-side. This problem was solved by removing bond wires which had made a short and by distributing the bias voltage drop over the oxide to both n- and p-sides. The detector of design B could be biased in the planned way with the full +70 V on the n^+ strips and the corresponding amplifiers at +4.5 V, thus dropping the full 65 V over 200 nm of oxide without any problems. In the following first preliminary results obtained with these detectors with a laser light spot, an ^{241}Am X-ray source and in a high energy test beam will be discussed.

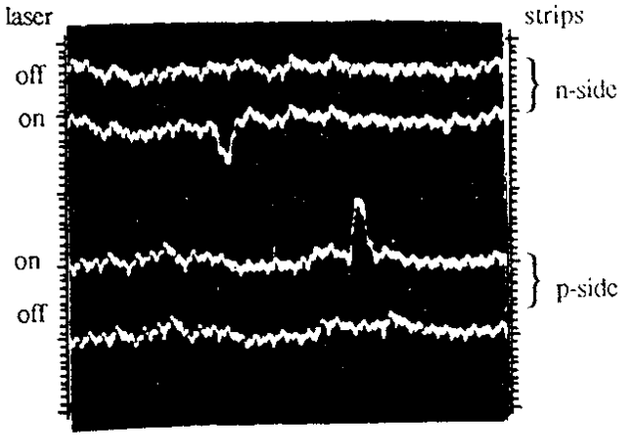

Fig. 5

A. Performance of the Detector with Thin Field-Plate Oxide

The laser pulse focussed to a diameter of about 50 μm could be observed on the oscilloscope very clearly both on the

n-side and the p-side, shining it onto the p-side (Fig. 5). The shape and the magnitude of the signals on both n- and p-side are very similar. Next the total charge of the pulse on the n-side was measured shining the laser light on the p-side as a function of depletion voltage (Fig. 6). Full depletion is reached around 60 volts.

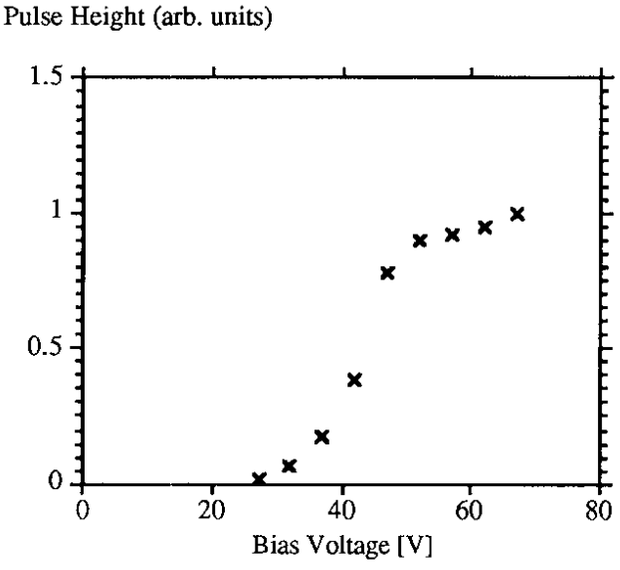

Fig. 6

To establish the confinement of the collected charge on the n-strips, a transverse scan with the laser was made across the n-strips shining on the p-side. The ratio of pulse heights $\eta = \frac{PH_i}{\sum_{i-2}^{i+2} PH_i}$ as a function of laser position starting the scan in position i-2 is shown in Figs. 7a and b. The curve in Figs. 7a and b are taken with depletion voltages and field-plate voltages of 45 V and -5 V and 55 V and -10 V respectively. One observes that the n^+ strips are separated ohmically for polarization voltages V between 5 to 10 volts. The distribution (Fig. 7b) looks very similar to the same distribution measured on the p-side (Fig. 7c).

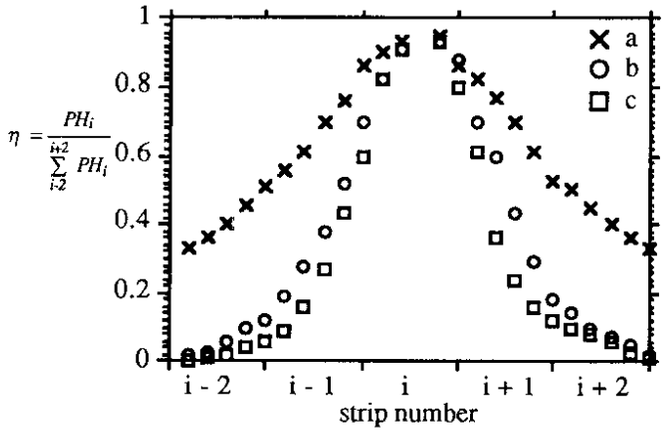

Fig. 7

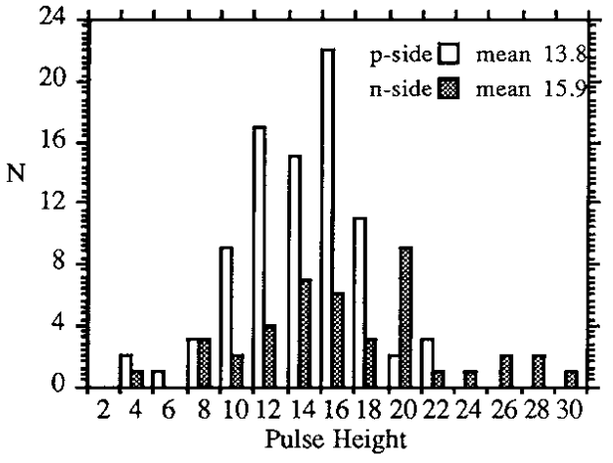

Fig. 8

Finally we exposed the detector to an Am X-ray source (60 keV). Selecting events which have strips on the p-side with a signal to noise ratio exceeding 5:1, we look for a signal on the n-side. The pulse height of the highest strip plus the pulse height of the neighbouring strip on each side are added. The total pulse height of signals on p- and n-side is shown in Fig. 8. Due to the limited speed of our on-line Macintosh computer, we read on p and n-side only 128 strips (out of 384) on which the Am source is centred. The Am source is wider than one chip and not focussed which explains the lower number of hits found on the n-side taking the p-side signals as a software trigger. The pulse height distribution for the Am signal is similar on p-side and n-side. The observed peak allows to extrapolate to a signal to noise ratio of about 12:1 for min.I. particles (84 keV energy deposition).

This detector was then put into a high energy π beam of 205 GeV at the CERN SPS. The n strips measured the vertical coordinate and the p strips the horizontal one. The impact point of a beam particle on this detector was defined by a telescope consisting of five 25 µm pitch DC-coupled Si microstrip detectors, 2 planes with vertical strips and 3 planes with horizontal strips. Only a small part of the data was useful, since this detector had many diode-metalstrip shorts on the p-side causing saturation over a wide range of readout channels on the p-side. During one run the beam was positioned on a relatively good region on the p-side with however the middle of the beam profile falling on a region of ~ 40 saturated channels. Nevertheless in these data 845 pulse height clusters created by a traversing beam particle were observed on the p-side, 372 clusters on the n-side with 194 coincident clusters. A cluster is defined by one strip with a pulse height greater than 2.5 r.m.s. noise, and any neighbouring strip with a pulse height greater than 1.5 r.m.s. noise. Clusters with more than 8 adjacent strips or a total pulse height less than 3.5 r.m.s. noise are rejected. The low number of clusters on the n-side and of coincident clusters is explained by the fact that at the edges of the bad p-region depletion does not penetrate fully to the n-side because of a voltage drop caused by high leakage currents in this region.

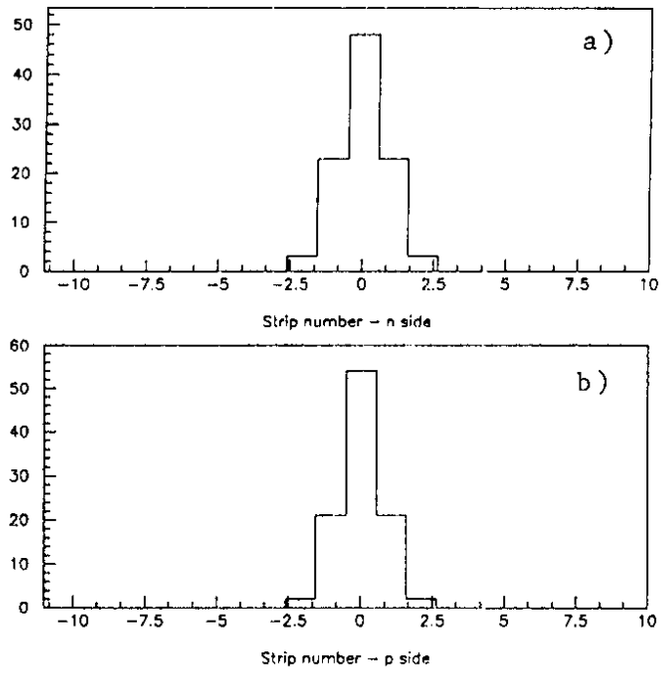

Fig. 9
Charge partition within clusters : a) n-side ; b) p-side

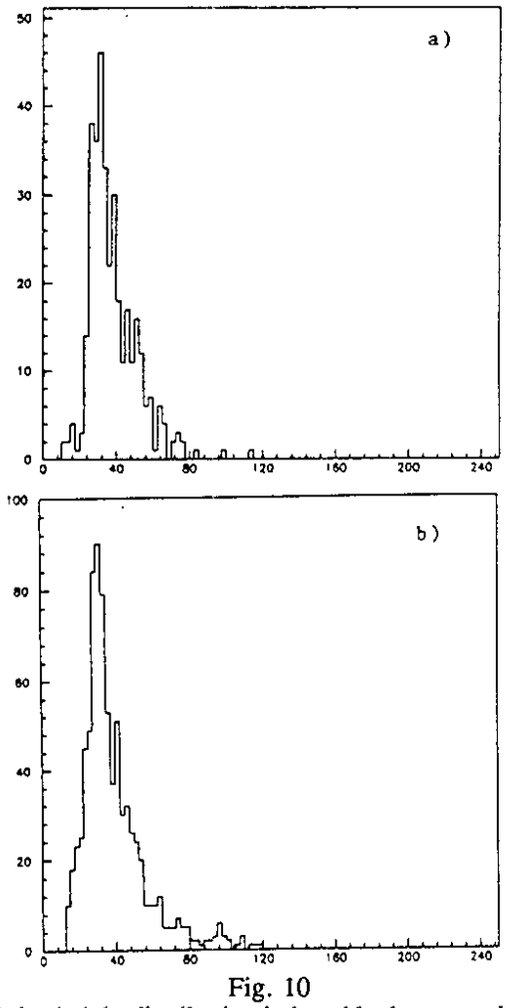

Fig. 10
Pulse height distribution induced by beam particles
a) n-side ; b) p-side.

Figures 9a and b show the charge partition between strips within clusters in percentage of the total charge with strip 0 being the highest one. As expected the charge on the n-side is slightly more spread out compared to the p-side. Figures 10a and b show the Landau distributions for the n-side and the p-side. The noise on the n-side is bigger (4.6 ADC counts) than on the p-side (3.7 ADC counts), due to the higher inter-strip capacitance caused by the wide metal strips (the beam was positioned in the area with 30 µm wide metal lines). The noise was bigger on both sides compared with the Am test conditions probably due to external pick-up in this test set-up. The average pulse height on n- and p-side is 31 and 30 ADC counts respectively, corresponding to signal to noise ratios of 6.6 and 8.1. Taking only the events with coincident clusters, we find S/N = 35 (n-side) and 33 (p-side). Figure 11 shows the Landau correlation of the 2 sides, indicating a concentration along the diagonal but very wide due to the relatively large noise. Figure 12 shows a plot of the beam profile with the 2 projections. The observed gap on the p-side is due to the diode-aluminium strip short in the centre of the beam. Residuals of the x and y coordinates with respect to the projected beam track could not be obtained due to a malfunction in the beam reference detectors.

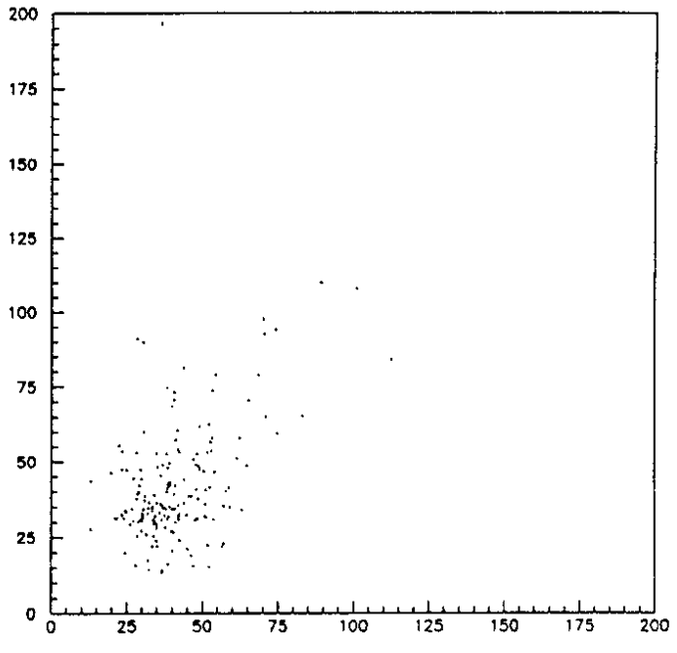

Fig. 11
Pulse height on n-side versus pulse height on p-side.

B. Performance of the Detector with Thick Field-Plate Oxide

The response of this detector to the laser light spot was the same as for the detector described above. Results from an exposure to the Am source are shown in Fig. 13. This detector could be operated in a way as foreseen in the design, with zero or small positive voltage between p-diodes and the input

input of the preamplifiers and full depletion voltage on the n^+ bias line. The whole depletion voltage is dropped over the thin oxide between n+ strips and metal lines. The bias voltage for the Am run was 50 V. The signal peaks at a signal over noise value of about 9 - independent of the cuts applied in the cluster search - leading to a signal to noise estimate for minimum ionizing particles of 12.5:1 for both sides.

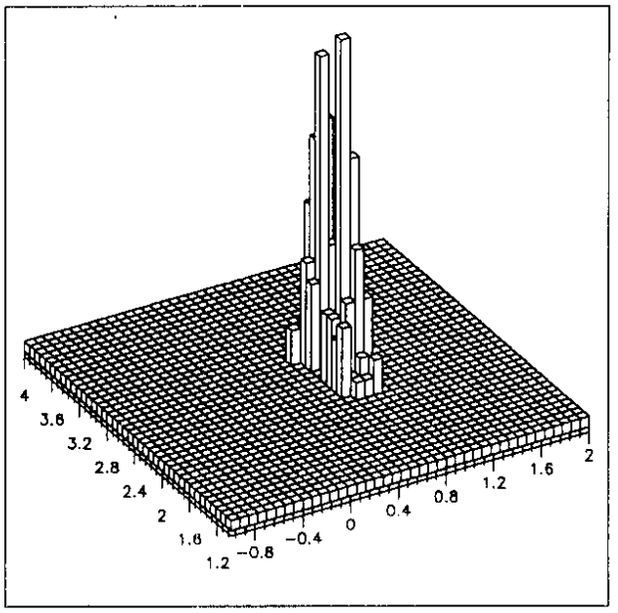

Fig. 12
Beam profile measured on both sides of detector.

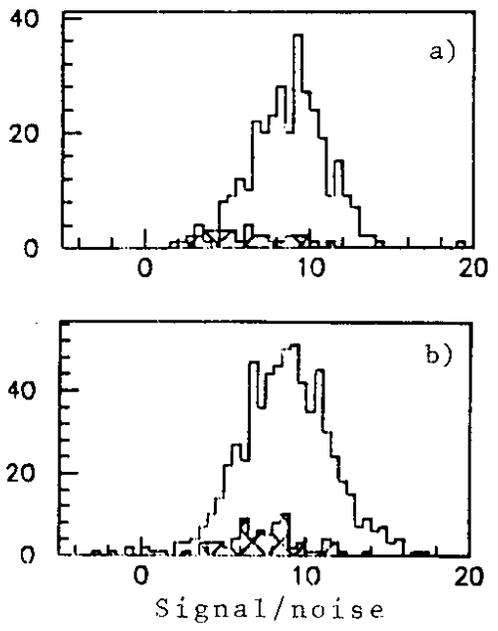

Fig. 13
241 Am pulse height spectrum for detector with thick field-plate oxide : a) n-side ; b) p-side.

This detector was subsequently tested in a 60 GeV beam at the CERN SPS. For this run a set of seven completely new reference detectors has been prepared. These were capacitively-coupled detectors with individual integrated bias resistors for each diode, 25 μm pitch, as used for the DELPHI microvertex detector [3], with a sensitive area of 60×32 mm^2. These detectors were equipped for readout with the NMOS VLSI chip [12]. Four of these detectors measured the horizontal co-ordinate (x) and three the vertical (y). The double-sided detector was installed in such a way that the n-side measured x and the p-side y. Figure 14 shows the beam profile as measured on the p-side and n-side. Figure 15 gives the Landau correlation and the projections. The peak of the pulse height distributions is found to be about 22 ADC counts. The average noise was found to be 1.8 and 2.8 ADC counts on the p-side and n-side respectively, giving a signal to noise ratio of about 12:1 and 8:1 respectively for beam particles. The increased noise level on the n-side compared with the Am run results are likely to be due to external noise pick-up.

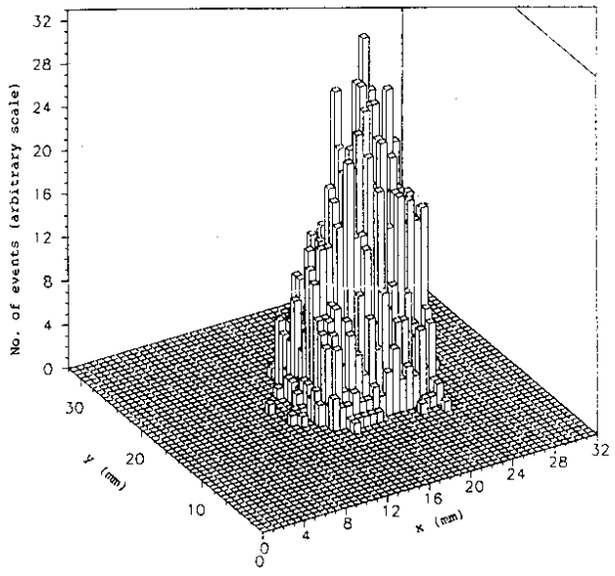

Fig. 14
Lego plot of beam profile from double-sided detector.

Figure 16 shows the cluster size distribution for both sides for the following cluster selection criteria : (i) At least one strip in the cluster has S/N > 2.5; (ii) all neighbouring strips with S/N > 1.5 are kept in the cluster. In Fig. 17 the residual distributions of the x and y-coordinates measured in the double-sided detector with respect to the track position fitted in the reference detectors and extrapolated to the double-sided detector are shown. Taking the FWHM of these distributions we find σ = 16 μm for both sides. It has to be emphasized that these results are very preliminary and a much more detailed analysis of the data is at present in progress. In

particular, the value of 16 μm for the spatial resolution can be considered as an upper limit.

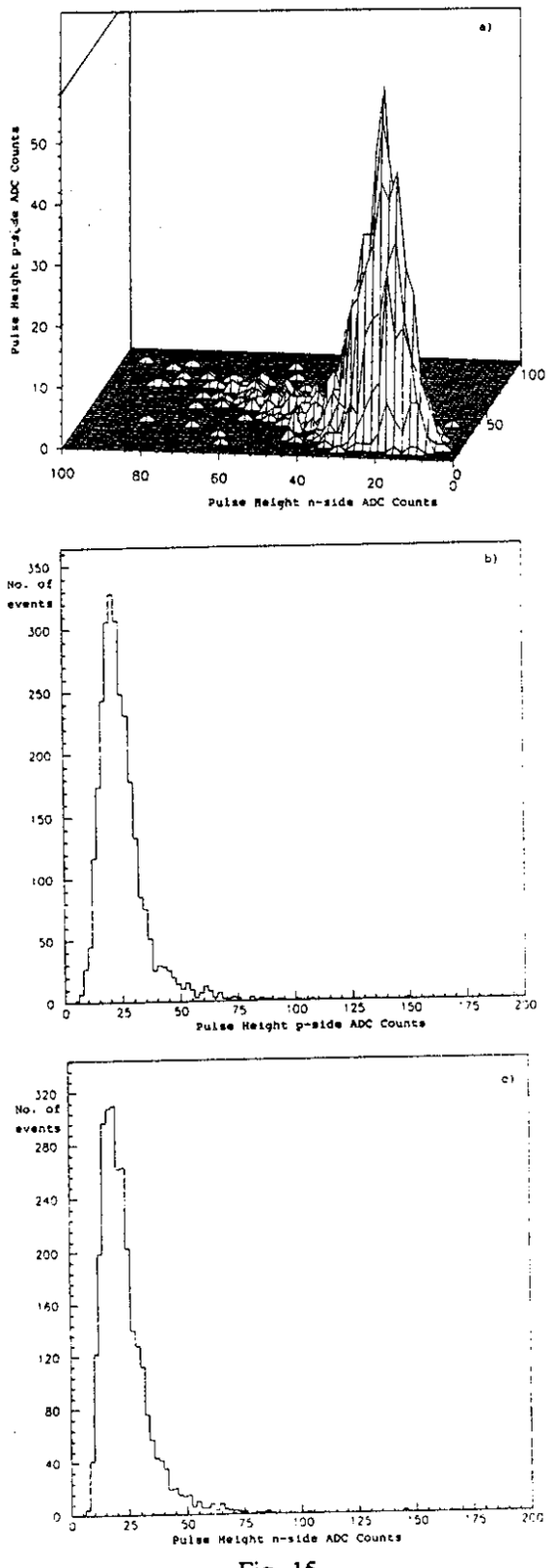

Fig. 15
Landau distributions on p- and n-side and their correlation from beam tracks.

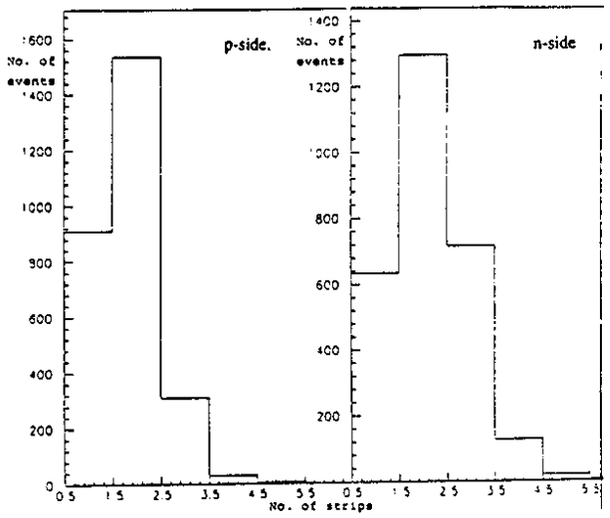

Fig. 16
Cluster size distributions for p-side and n-side.

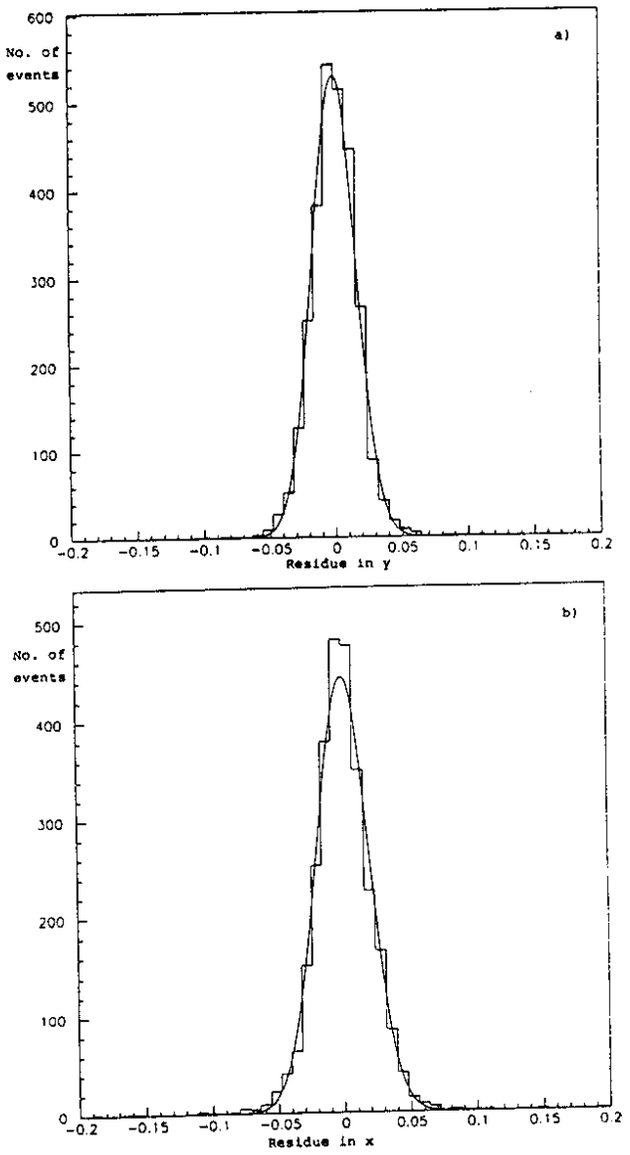

Fig. 17

6. CONCLUSIONS

Double-sided readout Si strip detectors with 50 μm strip pitch and readout pitch on each side have been built. These detectors have capacitive coupling of p^+ and n^+ strips to the readout strips and individual bias resistors. The ohmic separation on the n-side is achieved by creating a field-induced junction between n-strips using external field-plates. The detectors have been successfully tested in the lab with a laser light spot and an ^{241}Am source and show good confined charge collection both on p-side and n-side. Two detectors have been put in a high energy particle beam. They have shown good response to minimum ionizing particles on both the n-side and the p-side. A preliminary analysis of the spatial resolution gives σ = 16 μm on both sides. These results demonstrate that double-sided readout Si strip detectors can be used for experiments where spatial resolution in the 10 μm range is needed.

Acknowledgements

We would like to thank R. Boulter and K. Ratz for their excellent support in preparing and mounting these detectors. We would also like to thank N. Mayet for her effort with the software of the DAS and R. Fischer and R. Oswald for general mechanical support. We are extremely grateful to C. Ponting for typing the manuscript.

REFERENCES

[1] E.g. NA11/NA32 charm experiment at CERN SPS, Ω spectrometer at CERN SPS, E691 charm photo-production at Tevatron; see also, P. Weilhammer, *Proceedings of Workshop on New Solid State Devices for High Energy Physics*, Berkeley, California, USA, 1985, p.83.

[2] DELPHI Microvertex Detector, Addendum to DELPHI Technical Proposal DELPHI 86-86 GEN52 (Oct. 1986); See also : CDF Si Vertex Detector and MARK II μStrip Vertex Detector at SLC.

[3] V. Chabaud et al., "Test Beam Results from a Prototype for the DELPHI Microvertex Detector", to be submitted to *NIM A*.

[4] G. Batignani et al., *IEEE Trans. Nucl. Science,* Vol. 36, No. 1, Feb. 89;
G. Batignani et al., *NIM* A277, 147 (1989);
P. Holl et al., *IEEE Trans. Nucl. Science,* Vol. 36, No. 1, Feb. 89, p. 251;
H. Becker et al., *IEEE Trans. Nucl. Science,* Vol. 36, No. 1, Feb. 89, p. 246.

[5] P. Holl et al., *NIM* A257, 587 (1987).

[6] L. Evensen et al., "A Silicon Microstrip Detector with Integrated Coupling Capacitors and Polysilicon Biasing Resistors, *Proceedings of 4th International Conference on Solid-State Sensors and Actuators*, Tokyo, Japan, June 1987, p. 271.

[7] M. Caccia et al., *NIM* A260, 124 (1987).

[8] P. Seller et al., *IEEE Trans. Nucl. Science,* Vol. 35, No. 1, Feb. 88, p. 176.

[9] H. Dijkstra et al., *IEEE Trans. Nucl. Science,* Vol. 36, No. 1, Feb. 89, p. 591.

[10] Thesis by T. Tuuva, University of Helsinki, "Silicon Strip Detectors and VLSI Readout"; to appear.

[11] SIROCCO, "A Silicon Strip CAMAC Controller" CERN EP ELECTRONICS NOTE 86-01.

[12] T. Walker et al. *NIM* A260 (1987) 124.